

Electronic Supplementary Material

Facile Bottom-Up Synthesis of Graphene Nanofragments and Nanoribbons by Thermal Polymerization of Pentacenes

Yosuke Ishii,^a Hayong Song,^a Hidenori Kato,^b Masashige Takatori^b and Shinji Kawasaki^{*a}

^aDepartment of Materials Science and Engineering, Nagoya Institute of Technology, Gokiso-cho, Showa-ku, Nagoya 466-8555, Japan

^bKuroganekasei Co. Ltd., 87 Arajingiri, Nishinaka, Chiryu 472-0016, Japan

Experimental Details

Mass spectrum measurements of the obtained samples were conducted using a laser desorption/ionization time-of-flight (LDI-TOF) mass spectrometer (JEOL JMS-S3000) equipped with a 349-nm-wavelength UV laser as ionization source. The mass spectrometer was operated in positive-ion detection mode. The Measurements were performed without using any matrix. The m/z scales of obtained spectra were externally calibrated with the decomposition peak positions of polyethylene glycol (PEG). Metallic impurity of the initial pentacene sample was checked by elemental analysis data obtained by an energy dispersive X-ray (EDX) spectrometer equipped with a JEOL JSM-7001F scanning electron microscope (SEM). Raman scattering

spectra excited by 514.5 nm Ar laser were collected using a Raman microscope system equipped with the Princeton Instrument Acton SP2300 charge-coupled device (CCD) detector. X-ray diffraction (XRD) patterns of the obtained materials were collected using a Rigaku MiniFlex diffractometer using Cu K α radiation ($\lambda = 0.154$ nm) as an incident beam. Room-temperature photoluminescence spectra were obtained using JASCO FP8600 spectrometer. All measurements were performed at room-temperature.

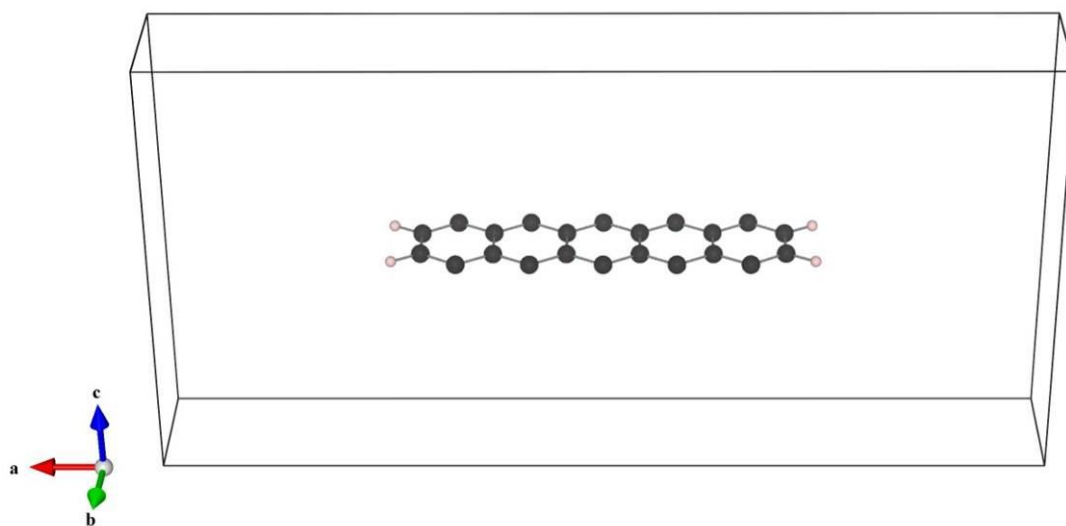


Figure S1. Unit cell structure of the pentacene-based GNR used for the calculation. ($a = 30.0 \text{ \AA}$,

$b = 4.26 \text{ \AA}$, $c = 15.0 \text{ \AA}$, $\alpha = \beta = \gamma = 90.0^\circ$)

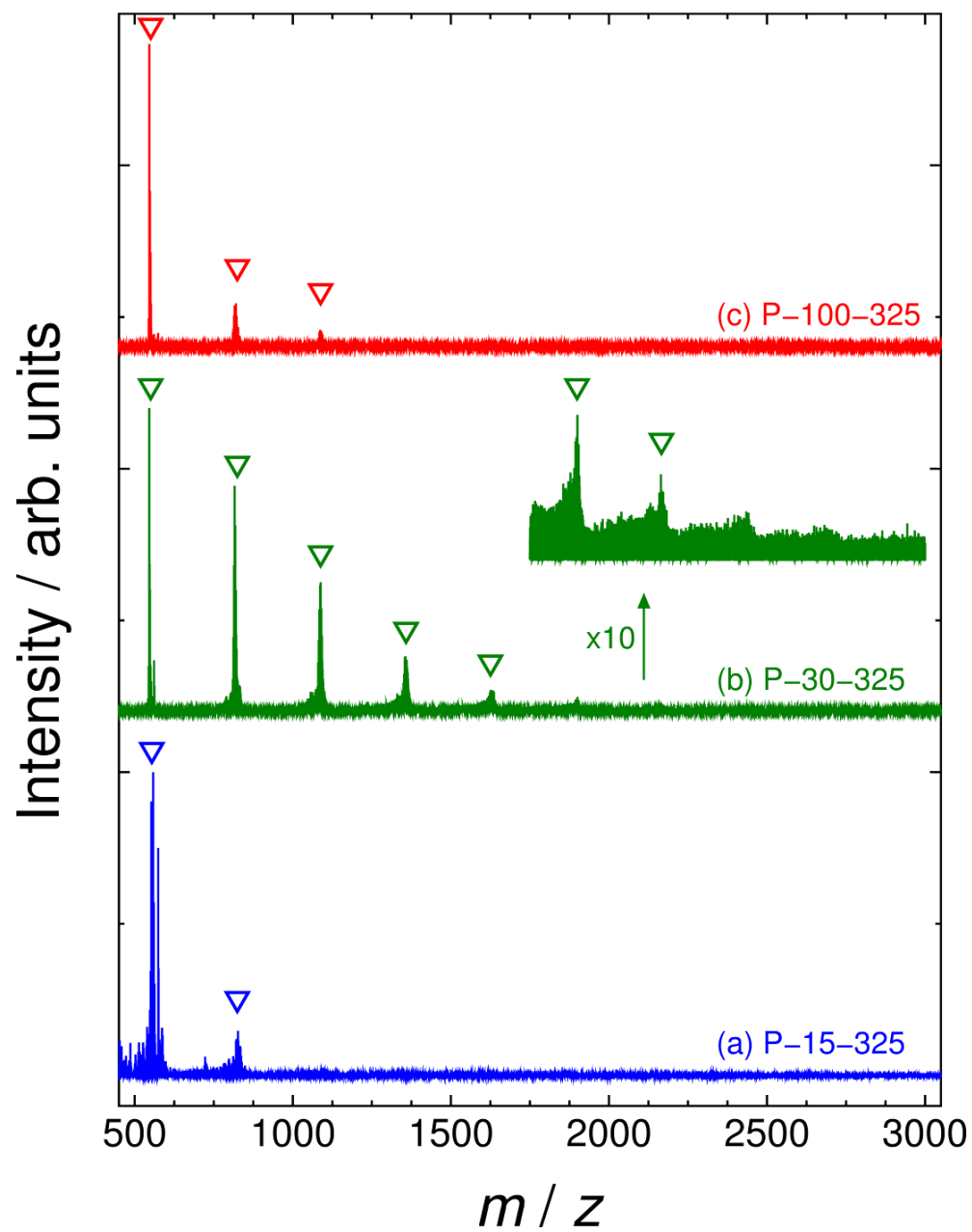


Figure S2. LDI-TOF mass spectra of the (a) FP-15-325, (b) FP-30-325, and (c) FP-100-325 samples.

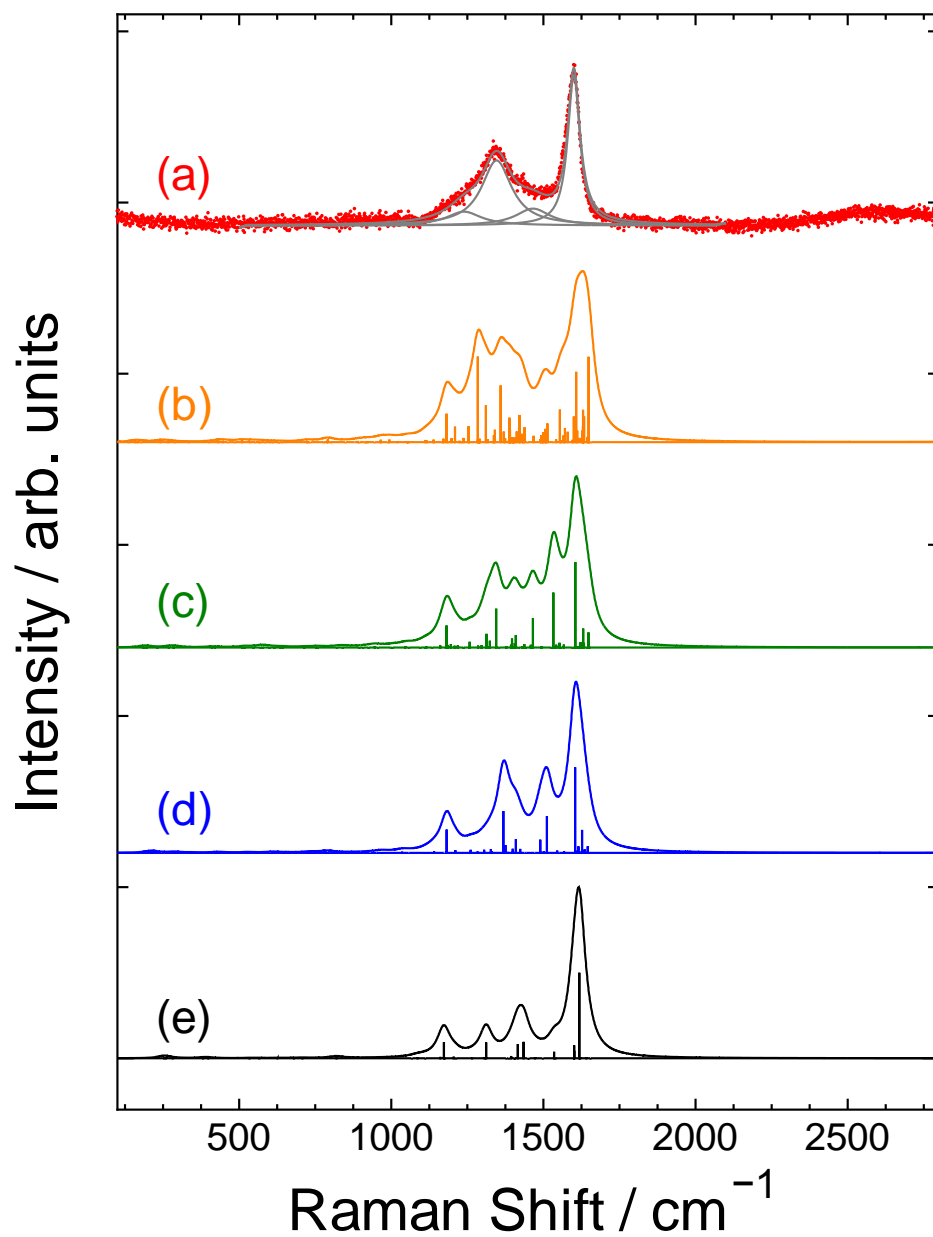


Figure S3. (a) Raman spectrum of the FP-30-325 sample. Simulation pattern of (b) pentacene pentamer (**4**, $n = 5$), (c) pentacene tetramer (**4**, $n = 4$), (d) pentacene trimer (**3**), and (e) pentacene dimer (**2**), that calculated by DFT B3LYP/cc-pVDZ method, are also shown in the figure.

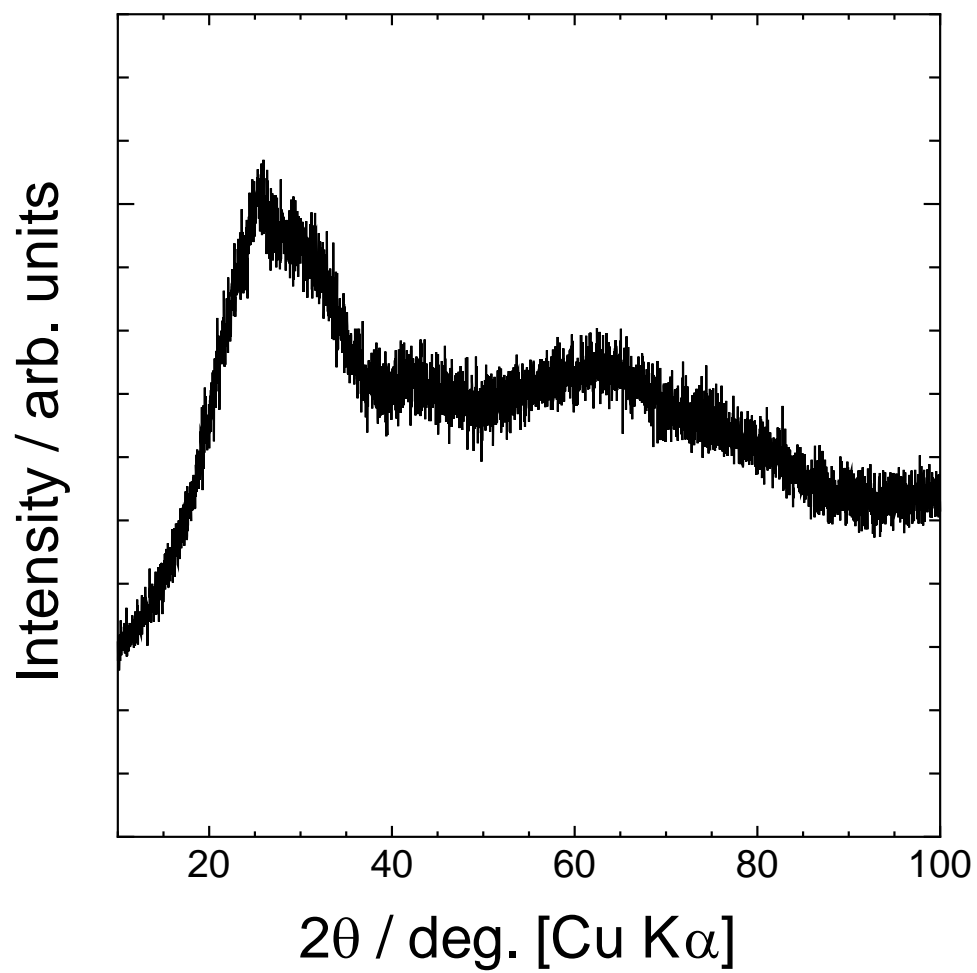


Figure S4. XRD pattern of the FP-30-325 sample. Cu K α radiation ($\lambda = 0.154$ nm) was used as an incident beam.

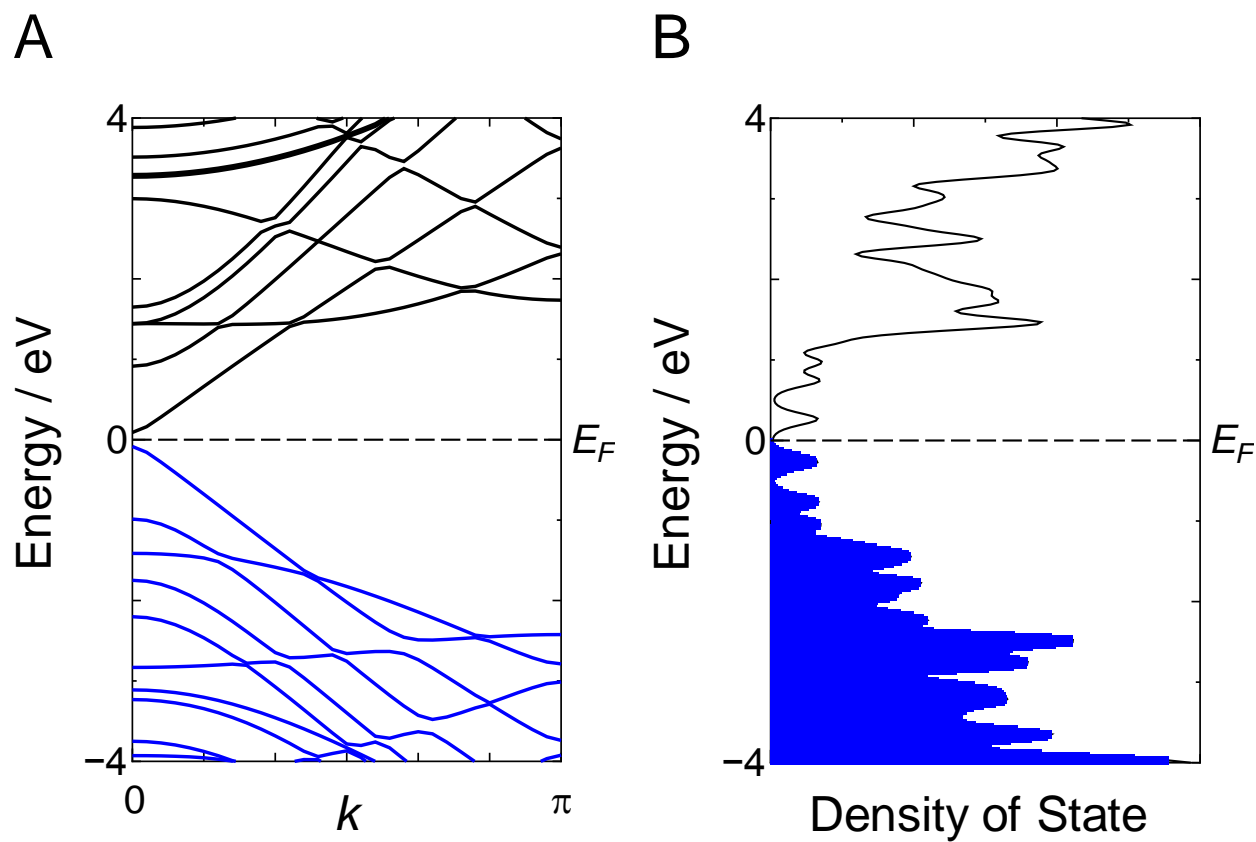


Figure S5. Calculated band structure (A) and DOS (B) of the pentacene-based GNR. In the DOS plot, the positions of Fermi energies (E_F) were set as 0 eV, and valence levels were filled with blue.

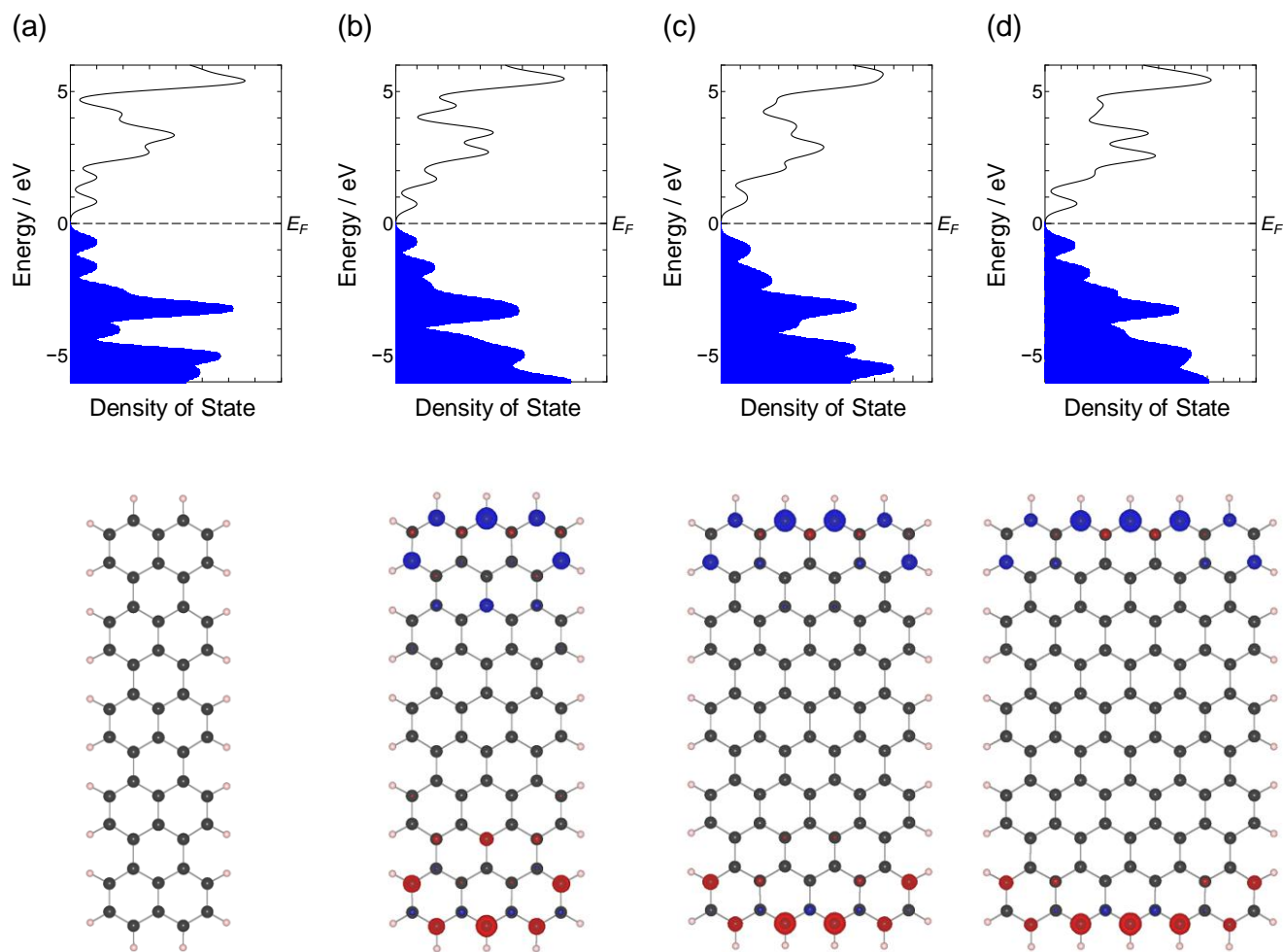


Figure S6. DOS (upper) and graphical representation of net spin-densities (lower) of (a) naphthalene pentamer, (b) anthracene pentamer, (c) tetracene pentamer, and (d) pentacene pentamer calculated by spin-unrestricted B3LYP/cc-pVDZ method. The DOS plots were obtained as the sum of Gaussian functions centered at molecular orbital energies with a full-width at half-maximum of 0.5 eV. In these figures, the positions of Fermi energies (E_F) were set as 0 eV, and valence levels were filled with blue. In the spin-density plots, red and blue regions represent excess α -spin density and excess β -spin density, respectively.

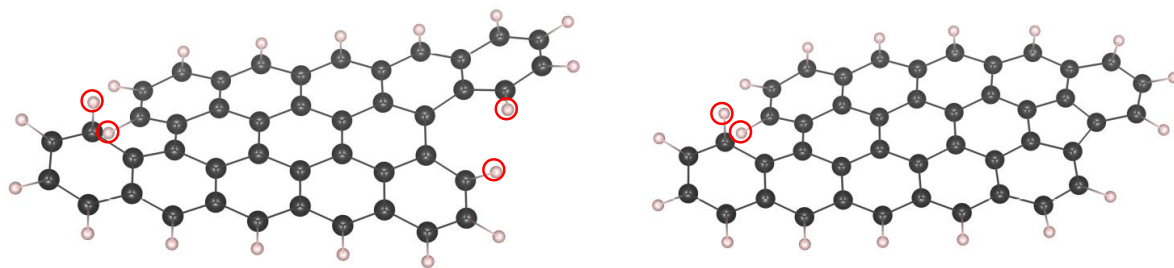


Figure S7. Three-dimensional molecular structure of C₄₄H₂₀ (**9**, left) and C₄₄H₁₈ (**10**, right).

Steric repulsions between hydrogen atoms placed at the shifted site were marked with circles.

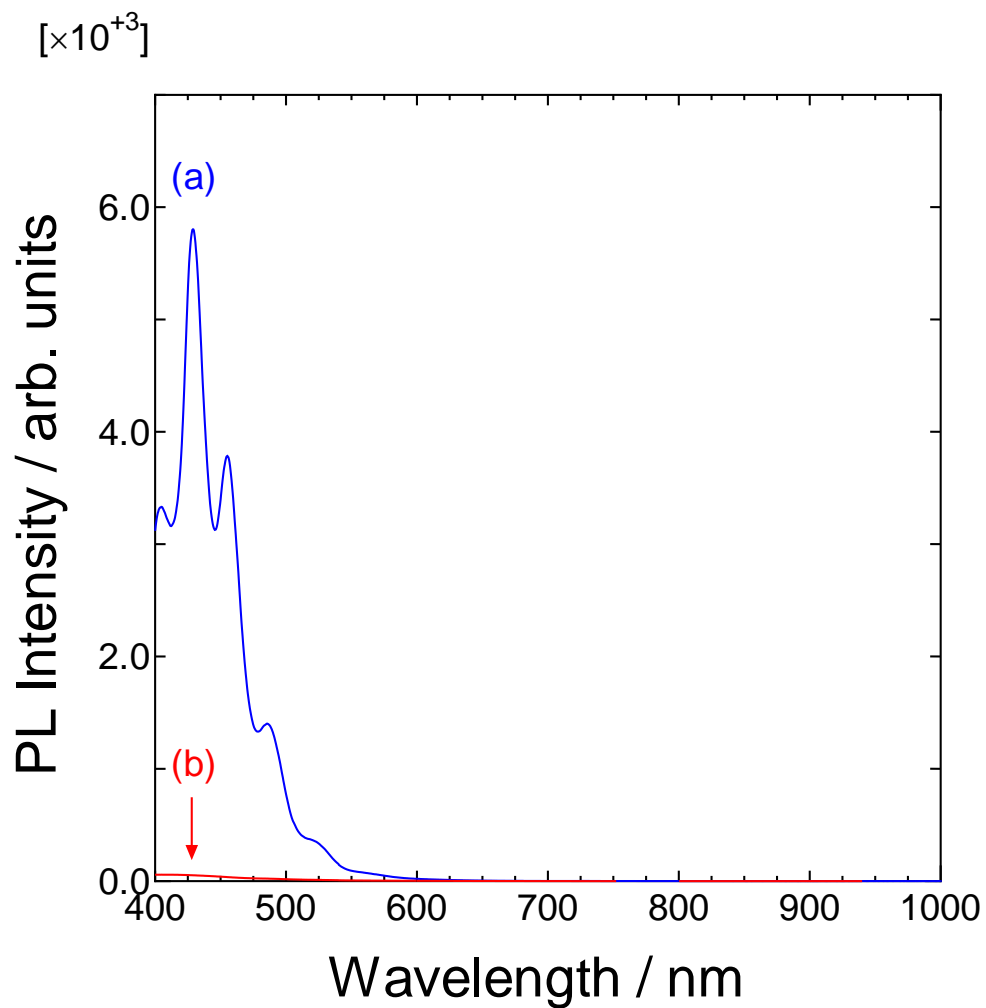


Figure S8. (a) Photoluminescent (PL) spectrum of the purified FP-30-325 sample dissolved in NMP. A monochromatic ultra-violet light ($\lambda = 365$ nm) was used for excitation source. In order to show background level, PL spectrum of the pure NMP is also shown in (b).

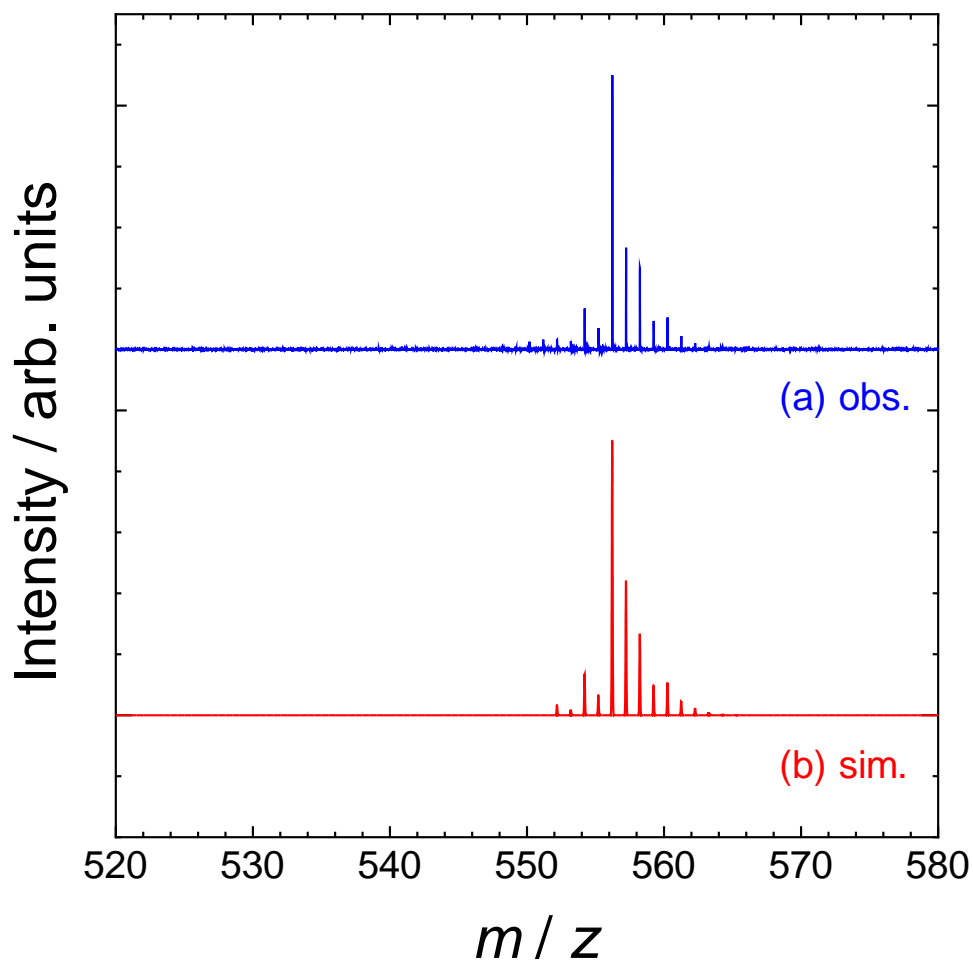


Figure S9. Magnified view of (a) observed and (b) simulated LDI-TOF mass spectra of soluble component of the FP-30-325 sample. In the spectrum simulation, the molecular composition was set to $C_{44}H_{24} : C_{44}H_{26} : C_{44}H_{28} : C_{44}H_{30} : C_{44}H_{32} : C_{44}H_{34} = 4 : 15 : 100 : 19 : 10 : 1$.

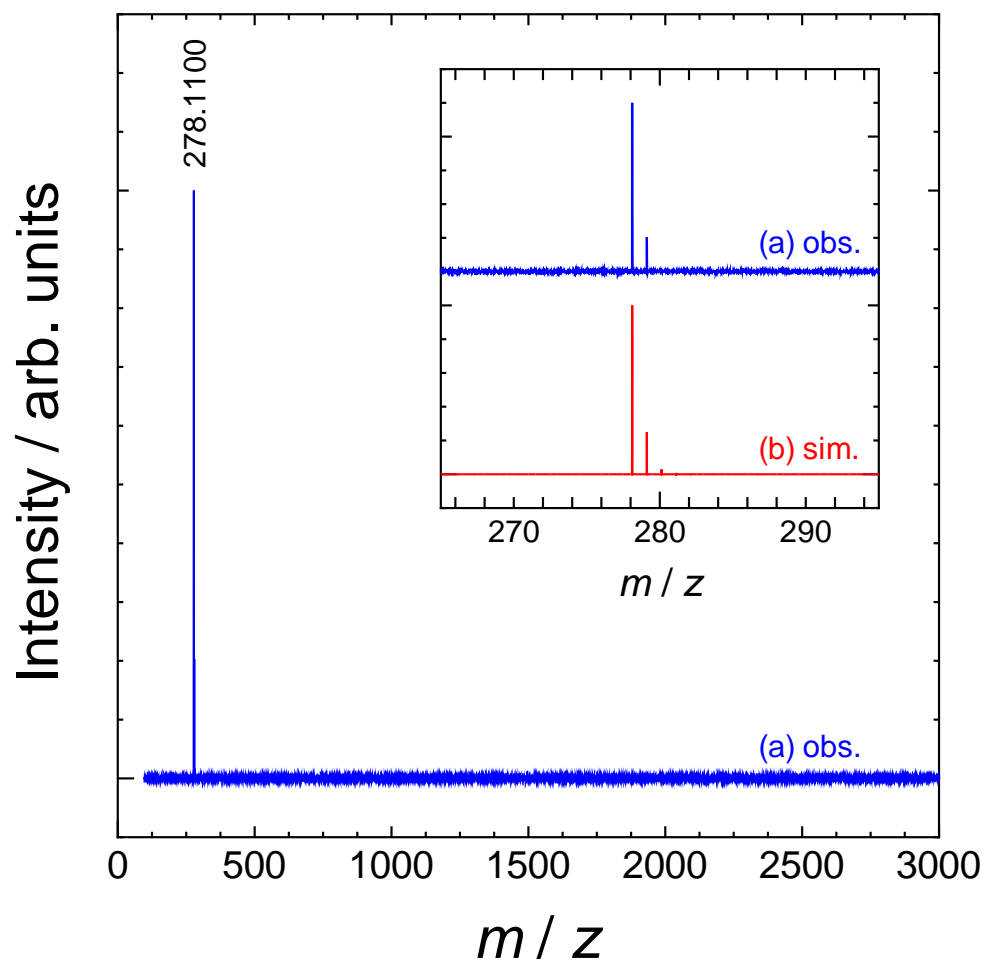


Figure S10. LDI-TOF mass spectrum of pentacene sample that used for the fusing reaction. The observed spectrum (a) was completely-consistent with the simulated isotope pattern of C₂₂H₁₄ (b).

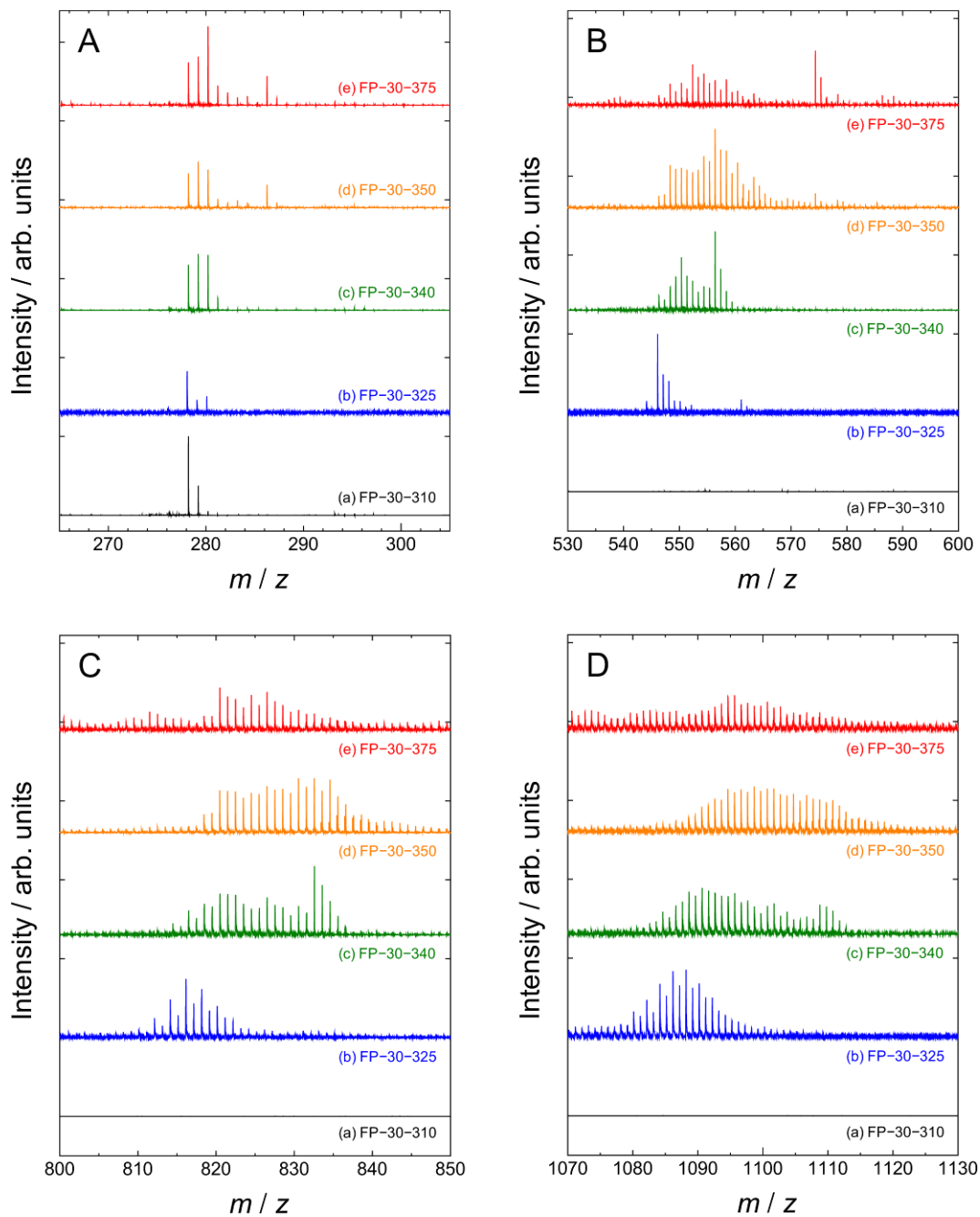


Figure S11. Detailed LDI-TOF mass spectra (magnified view of Figure 1) of the (a) FP-30-310, (b) FP-30-325, (c) FP-30-340, (d) FP-30-350, and (e) FP-30-375 samples. The pentacene monomer ($n = 1$), dimer ($n = 2$), trimer ($n = 3$), and tetramer ($n = 4$) regions are separately shown in A, B, C, and D, respectively.

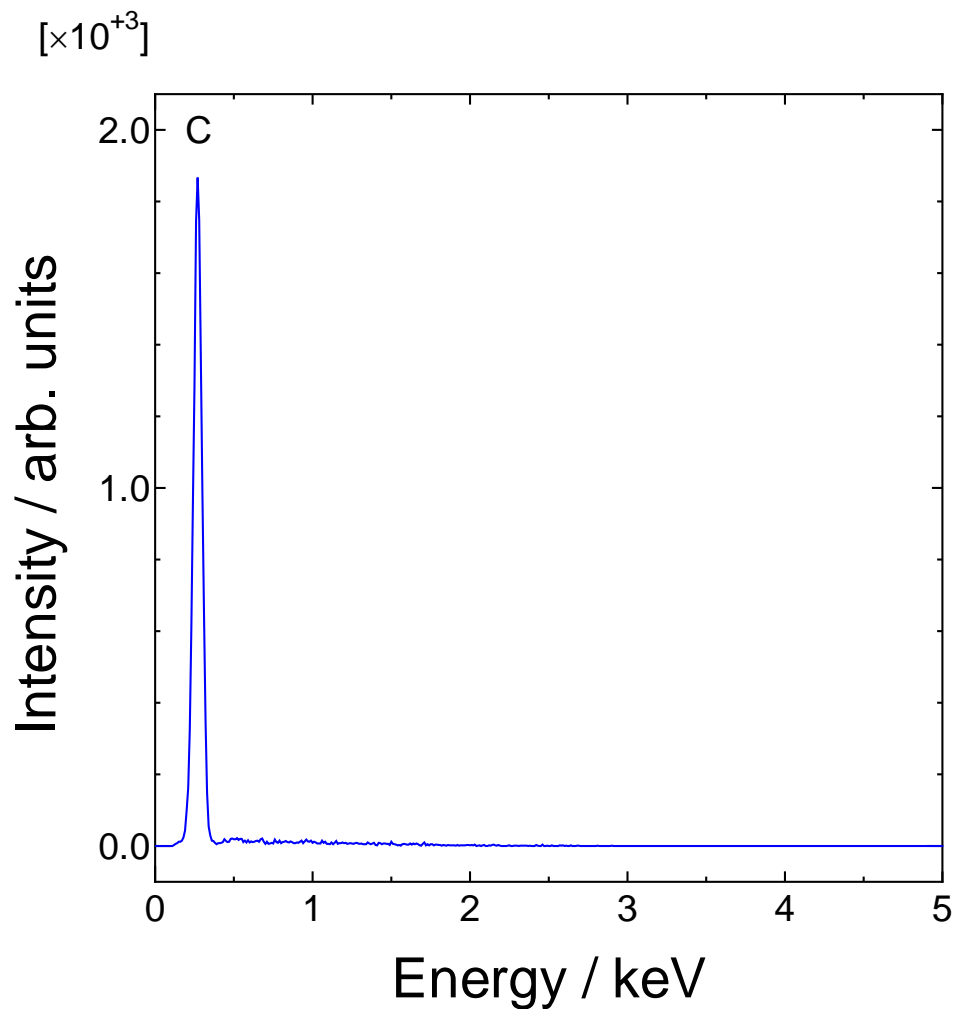


Figure S12. EDX spectrum of the pentacene sample that used for the fusing reaction.

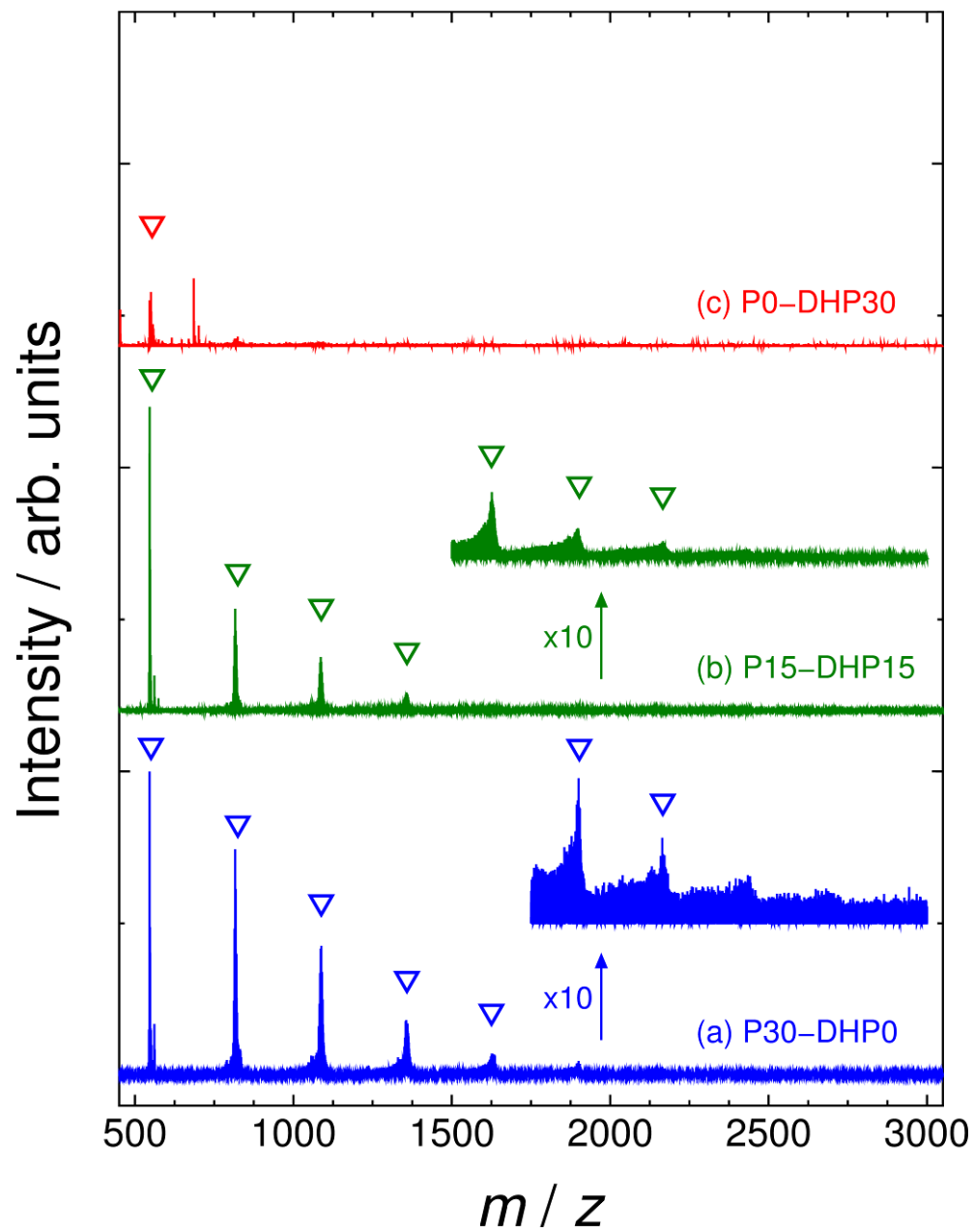


Figure S13. LDI-TOF mass spectra of the (a) P30-DHP0, (b) P15-DHP15, and (c) P0-DHP30 samples.